Some Backscatter Modeling Issues Complicating the Sonar-Based Monitoring of Suspended Sediments in Rivers

Adrien Vergne, Jérôme Le Coz, Céline Berni

AGU ADVANCING EARTH AND SPACE SCIENCE

Water Resources Research

RESEARCH ARTICLE
10.1029/2022WR032341

Some Backscatter Modeling Issues Complicating the Sonar-Based Monitoring of Suspended Sediments in Rivers

Adrien Vergne[1], Jérôme Le Coz[1], and Céline Berni[1]

[1]INRAE, UR RiverLy, Villeurbanne, France

Key Points:

- Modeling the acoustic backscatter of suspended sediments in rivers often results in large errors
- Various sources of error may arise from the diversity and complexity of scatterers in rivers
- Specific experiments and theoretical developments are required to identify and reduce modeling errors

Correspondence to:

J. Le Coz,
jerome.lecoz@inrae.fr

Citation:

Vergne, A., Le Coz, J., & Berni, C. (2023). Some backscatter modeling issues complicating the sonar-based monitoring of suspended sediments in rivers. *Water Resources Research*, *59*, e2022WR032341. https://doi.org/10.1029/2022WR032341

Received 9 MAR 2022
Accepted 2 JUN 2023

Abstract The measurement of suspended sediments from acoustic backscatter was originally developed in marine science for monitoring near-bottom suspensions usually composed of sand particles. In the last decade, there has been a growing interest in adapting these techniques to rivers. The so-called "solid particle theory" developed in oceanography mainly applies to suspensions of non-cohesive solid particles producing incoherent backscatter signal. So far, this theory has been used for interpreting river backscatter even if it relies on assumptions that are not obviously met in rivers. This study uses a set of measurements made on the Rhône River in France to discuss the typical issues which challenge the interpretation of sound backscattering for monitoring suspended sediments in rivers. Large discrepancies between model outputs and measurements for frequencies lower than 2.5 MHz suggest that other scattering processes including flocculation and air micro-bubbles may have a large impact on acoustic backscatter and attenuation. Deviations of the backscatter echo distribution from Rayleigh statistics were observed, suggesting that the assumption of incoherent backscattering is not always met. This work calls for the development of a more complete theory for interpreting river backscatter.

1. Introduction

Measuring suspended sediment fluxes in rivers is crucial for a range of river science and engineering applications. Suspended sediments in rivers often show a bimodal particle size distribution (PSD), with a fine sediment mode composed of silt and clay particles, and a coarser mode composed of sand particles (Agrawal & Hanes, 2015; Armijos et al., 2017). Estimating the suspended sediment load typically requires measuring the suspended sediment concentration (SSC) throughout the river cross-section. Traditionally, SSC has been measured by collecting water samples (Gray & Landers, 2014). However, a major limitation of water sampling techniques is their poor spatial and temporal measurement resolution. When SSC is not steady and homogeneously distributed throughout the river cross-section, the poor resolution of water sampling techniques can lead to large errors in the sediment load estimation, in particular regarding the sand mode (Grams et al., 2018).

Hydroacoustic science is a promising field of research for increasing SSC measurement resolution in rivers, using active sonars that emit a pulse of sound, called a "ping," and receive its reflections (echoes). The device that emits and receives sound is called a transducer. The so-called "sonar beam" is commonly defined as the area where the acoustic power is at least 50% (i.e., −3 dB) of the maximum power found in the transducer axis. In water, the sound is scattered in all directions by objects in suspension (the scatterers) and the sound that travels back to the transducer is the backscatter. Knowing the speed of sound, which can be computed from water temperature, pressure and salinity, the distance to the scatterers can be deduced from the return time of the ping. Thus, it is possible to relate signal time windows to ensonified volumes or "sonar cells" along the sonar beam, which allows to measure backscatter profiles. The strength of the signal backscattered from a sonar cell is determined by the number and type of scatterers in that cell, and by the acoustic attenuation by water and suspended particles all along the acoustic path between the transducer and the cell.

Hydroacoustic techniques were originally developed in acoustical oceanography for measuring near-bottom sediment suspensions (Hay, 1983). In the last four decades, acoustic scattering models have been significantly improved with a focus on sand suspensions and marine applications (Hay, 1991; Hay & Sheng, 1992; Sheng & Hay, 1988; Moate & Thorne, 2012; Moate et al., 2016; Thorne & Buckingham, 2004; Thorne & Hardcastle, 1997; Thorne & Meral, 2008; Thorne et al., 1993, among others). More recently, the success of Acoustic Doppler Current Profilers (ADCP), specific sonars used for measuring river depth, velocity and discharge, has boosted the interest in adapting SSC measurement techniques developed in oceanography to river environment. In particular,

much progress has been made in the last decade in continuously monitoring fine and sand SSCs across the river width using side-looking ADCPs (Moore et al., 2013; Topping & Wright, 2016; Topping et al., 2007, among others). Side-looking techniques assume suspension homogeneity along the sonar beams and require in situ calibration through water sampling. If one of these conditions is not met, retrieving the SSC from the sonar signal becomes much more difficult.

As specific acoustic backscatter and attenuation models do not exist yet for interpreting the sonar signal in a fluvial environment, the theoretical background developed in acoustical oceanography has been used in most studies conducted in rivers until now (Baranya & Józsa, 2013; Hanes, 2012; Haught et al., 2017; Holdaway et al., 1999; Landers et al., 2016; Latosinski et al., 2014; Moore et al., 2012, 2013; Reichel & Nachtnebel, 1994; Sassi et al., 2012, 2013; Szupiany et al., 2019; Topping & Wright, 2016; Venditti et al., 2016; Vergne et al., 2020; Wright et al., 2010). In the present paper, this theoretical background is called "the solid particle theory," as the suspended particles are supposed to be non-cohesive and made of solid material. This theory was summarized by Thorne and Hanes (2002) and Thorne and Hurther (2014).

Even if it has been largely used in many fluvial studies, it is not obvious that the solid particle theory can predict the backscatter signal recorded in a river as well as it does in some marine environments. Actually, some complications were identified early in the development of acoustic SSC monitoring techniques, even in the ocean. For example, Hanes et al. (1988), Vincent et al. (1991) and many subsequent papers discussed complications due to near-field corrections, air bubbles, sediment size variations, inversion instabilities, organic matter, and instrument noise levels. Those papers and several others also suggested that laboratory calibration using sediment samples collected in the field was generally required because a calibration only based on theory was simply not sufficiently accurate.

This paper intends to help dispel the growing misconception that it is easy to measure the SSC profile in a river using a commercial mono-frequency ADCP or even a multi-frequency Acoustic Backscatter System (ABS) primarily designed to record backscatter profiles. Whatever the deployment mode and site conditions, the operator must be aware of typical difficulties that challenge the interpretation of sound backscattering in rivers. These difficulties are reviewed in this paper in order to help other users understand their measurements and to suggest future researches addressing the current limitations of the technique. The present article does not intend to criticize the existing theory nor present any new theory or method. The objective is rather to: (a) show that important discrepancies may exist between the predictions of the solid particle theory and the backscatter signal recorded in a river; (b) open a discussion, on the basis of currently known physical processes, to support research perspectives in order to understand the causes of these discrepancies and develop methods to handle them. While inversion algorithms are beyond the scope of this paper, the final goal is to improve hydroacoustic inversion techniques in rivers.

The rest of the paper is organized as follows. Section 2 is a reminder of the theoretical basis necessary to understand the specific issues discussed in this paper. Section 3 presents the typical data set used in this study to illustrate the error sources, a set of water samples and acoustic measurements acquired with a multi-frequency ABS on the Rhône River in France at various experimental sites, for diverse sediment load conditions. Observations and modeling results are presented in Section 4. In Section 5, error sources that could explain the observed discrepancies between modeled and measured backscatter and/or the observed deviations from Rayleigh statistics are reviewed and discussed. Finally, after concluding on the identified error sources and their impacts on the sonar-based monitoring of suspended sediments in rivers, some possibilities of improvement are discussed.

2. The Solid Particle Theory

2.1. Assumptions and Sonar Equation

The solid particle theory is based on the following assumptions: (a) sound scattering in the ensonified volume is only due to non-cohesive solid particles; (b) the suspended particles occupy random positions from ping-to-ping, which leads to random phases and incoherent backscatter signal; and (c) there are enough particles of each type in the ensonified volume.

Under these assumptions, the sonar equation that describes the acoustic backscatter signal, linearly proportional to the pressure at the transducer, recorded by a calibrated monostatic sonar system in the presence of suspended scatterers can be written as (Thorne & Hanes, 2002; Thorne & Hurther, 2014):

$$\overline{V^2} = \frac{16\pi}{3}\frac{k_t^2 s_v}{\psi^2 r^2} e^{-4r(\alpha_w+\alpha_s)} \tag{1}$$

where V (Volts) is the amplitude of the voltage recorded by the sonar instrument in one sonar cell, $\overline{V^2}$ is the quadratic average of V over many sonar pings, k_t (V m$^{3/2}$) is the instrument calibration constant described by Betteridge et al. (2008), s_v (m^2 m^{-3}) is the volume backscattering coefficient (Medwin & Clay, 1998), r (m) is the range from the transducer, ψ is a near-field correction (Downing et al., 1995), α_w (m^{-1}) is the acoustic attenuation due to water viscosity and α_s (m^{-1}) is the attenuation due to the suspended particles. As all the measurements in this study are made in the far field of the transducers, the near-field correction will be ignored ($\psi = 1$). Water attenuation (α_w) was computed from water temperature using the François and Garrison (1982) formula.

2.2. Acoustic Backscatter and Attenuation

In Equation 1, two parameters depend on the suspension: s_v, that describes the strength of the echo produced by an ensonified volume of the water column located at range r from the transducer; and α_s, that describes the acoustic attenuation due to the suspended particles along the acoustic path. In the solid particle theory, s_v and α_s are expressed as:

$$s_v = \frac{3M(r)}{16\pi}\frac{\int_0^\infty a^2 f_\infty^2(a) n(a) \mathrm{d}a}{\rho_s \int_0^\infty a^3 n(a) \mathrm{d}a} \tag{2}$$

$$\alpha_s = \frac{1}{r}\int_0^r \frac{3\int_0^\infty a^2\left[\chi_{ss}(a) + \chi_{sv}(a)\right] n(a)\mathrm{d}a}{4\rho_s \int_0^\infty a^3 n(a)\mathrm{d}a} M(r) dr \tag{3}$$

where M (kg m^{-3}) is the SSC in the sonar cell:

$$M(r) = N(r)\frac{4\pi\rho_s}{3}\int_0^\infty a^3 n(a)\mathrm{d}a \tag{4}$$

and N is the total number of scatterers in the sonar cell, a (m) is the particle radius, $n(a)$ is the particle radius number probability density function, ρ_s (kg m^{-3}) is the density of the particle constituent material (assumed to be constant), r (m) is the range from the transducer, f_∞ is the form factor that describes the basckattering properties of the particles, and χ_{ss} and χ_{sv} are the total normalized scattering and viscous cross-sections, respectively, that describe acoustic energy losses due to, respectively, sound scattering by the suspended particles, and energy dissipation in the viscous sublayer of the fluid around the particles when they are moved by the acoustic wave. Note that in the above equations, M, N, and $n(a)$ depend on range r, as the sediment suspensions examined in this study are usually not homogeneous along the acoustic path.

In the following, we used SSC and PSD data derived from water samples to compute s_v and α_s from Equations 2 and 3, using f_∞ and χ_{ss} models described in Thorne and Meral (2008), and the χ_{sv} model described in Urick (1948). These models have been previously used in many ocean and river studies. The volume density $n_v(a)$ provided by laser grain-sizers has been converted to number density $n(a)$ assuming that particles are statistically spheric as explained by Vergne et al. (2021):

$$n(a_i) = \frac{1}{\Delta a_i}\frac{n_v(a_i)/a_i^3}{\sum_i n_v(a_i)/a_i^3} \tag{5}$$

where a_i (m) is the radius of the ith size class of the laser grain-sizer and $\Delta a_i = a_{i+1} - a_i$.

2.3. Echo Statistics

As in most sonar applications, the backscatter pressure produced by a suspension of particles is of statistical nature. The backscatter recorded by the instrument is the sum of all individual echoes produced by the scatterers within the ensonified volume, that is, one sonar cell. These individual echoes interact in a constructive or destructive way, that is, in-phase or out-of-phase. As the positions of the scatterers vary in space and time, the magnitude of the resulting backscatter recorded by the instrument fluctuates from one sonar cell to another and from ping to ping. Some authors called this signal variability "configurational noise" (Libicki et al., 1989) as it depends on the configuration of the positions of the scatterers.

We usually assume (a) that the scatterers within an ensonified volume at any instant in time are independent and therefore have random phases in the backscattered pressure wave, and (b) that each ping is an independent realization such that the phase of the return from an individual particle is random from ping to ping. When summing many sinusoids with same frequency, similar amplitudes, and random phases equally distributed over [0, 2π], the amplitude of the resulting wave is a random variable that varies from ping to ping. As a consequence of the Central Limit Theorem, this random variable follows a Rayleigh distribution (Siddiqui, 1962). Therefore, the backscatter signal produced by a suspension of many similar scatterers with random positions is theoretically Rayleigh-distributed. This was confirmed experimentally for suspensions of solid particles with narrow PSD (Thorne & Campbell, 1992; Thorne et al., 1993). The probability density function of a Rayleigh distribution is:

$$\mathrm{pdf}(V,\gamma) = \frac{2V}{\gamma}\mathrm{e}^{-V^2/\gamma} \tag{6}$$

where V is, in our case, the backscatter signal amplitude (voltage) recorded by the ABS, and γ is the Rayleigh distribution parameter. The best way to estimate γ is to measure the quadratic mean of the variable (V) over many realizations (sonar pings): $\gamma \approx \overline{V^2}$ (Siddiqui, 1962). Theoretically γ is also equal to the quadratic sum of the amplitudes of all individual backscattering echoes ($\gamma = \sum_i V_i^2$ where V_i is the voltage amplitude of each individual echo). The sonar equation (Equation 1) actually relies on this important property. However, this property may not be true if the assumptions that lead to Rayleigh echo distribution are challenged, for example, when the scatterers do not have random positions or when the number of dominant scatterers in the ensonified volume is too small. Although a Rayleigh-distributed sonar signal is a prerequisite to the application of the solid particle theory, signal statistics have not been inspected in river studies.

3. Data Set

3.1. Experimental Strategy

To study the validity of acoustic theory assumptions, this study focuses on the direct problem (modeling the sonar signal from the physical theory) and compares the reconstructed sonar signals with the measured sonar signals. Comparing SSC profiles rather than sonar signals would have needed to inverse the acoustic signals and compare the computed SSC outputs with the SSC measured from water samples. Acoustic inversion is a complex non-linear problem and may bring many large errors hindering the identification of issues in acoustic theory assumptions.

The data set used in this paper is built on specific measurements that we have conducted to study backscatter profiles acquired in typical river suspensions with an acoustically calibrated, multi-frequency ABS. Compared to more common single-frequency ADCP records, instrument constants are known for each frequency from manufacturer's calibration. Specific efforts intended to minimize acoustic, positioning, water sampling and sediment analysis errors which remain unavoidable in field conditions.

Data were collected at seven experimental sites on the Rhône River in France, between 2016 and 2018. We were able to observe various levels of SSC ranging from ~0.03 to ~10 g/l. Figure 1 shows a map of the experimental sites, the dates of data collection, and the approximate SSC levels.

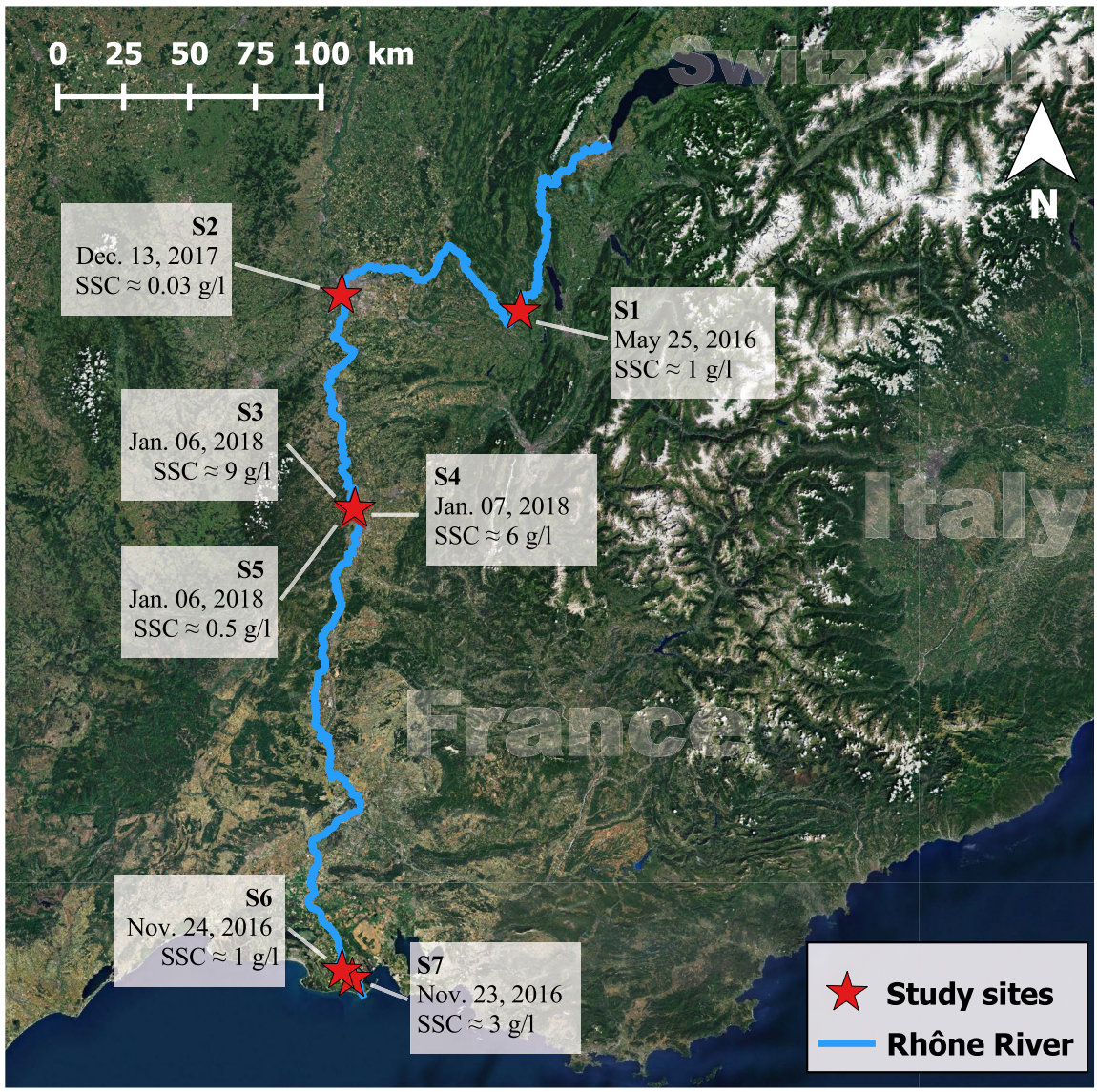

Figure 1. Map of the experimental sites. Labels indicate the site reference (e.g., S1), the date of data collection and an order of magnitude of the level of suspended sediment concentration in the water column.

3.2. Acoustic Measurements

At each experimental site, the backscatter signal throughout the water column was measured using an Aquascat 1000R ABS. The Aquascat 1000R is the best ABS commercially available for now that is suitable for field deployment. It is far better than ADCPs that have been commonly used in rivers for this type of studies until now: it is calibrated, it has multiple frequencies, we have access to much more parameters. This instrument has been successfully used in laboratory experiments by experienced research teams (e.g., Thorne et al., 2014). In our own laboratory tank (see Vergne et al., 2021), we found that its response was linear with range for homogeneous suspensions. However, information on the linearity of the instrument response to acoustic pressure over the full measurement range is not provided by the manufacturer, and it would require specific and expensive laboratory equipment to measure it. In theory the Aquascat data V varies between 0 and 1. By measuring the echo of an acoustic tile in a laboratory tank at various distances between the tile and the transducers, we observed the beginning of saturation for $V > 0.7$. Accordingly, we remove all the first cells of the sonar profiles where $V > 0.5$ to avoid any risk of saturation. We also intended to avoid non-linearity at low signal strength by using acoustic measurements with high Signal to Noise Ratio (at least SNR > 10) in the results presented in Sections 4.2 and 4.3.

Four frequencies were used at the same time and up to six frequencies were spanned using the transducers alternatively: 0.3, 0.5, 1.0, 2.5, 4.0, and 5.0 MHz. The instrument was previously calibrated by the manufacturer on a quasi-uniform suspension of glass beads of known size following Betteridge et al. (2008) procedure. The obtained k_t values are provided in Appendix A. Based on Betteridge et al. (2008) results, the expected accuracy of these values is about $\pm 10\%$. However we do not have access to precise information on the calibration operation like raw acoustic signal (the signal had been already averaged by the manufacturer), test of spatial and temporal suspension homogeneity, etc. As the vast majority of ABS users unfortunately, we have no access to a calibration tank to conduct a more precise and reliable calibration.

The instrument was deployed down-looking at the free-surface from a boat. Hundreds to thousands of individual sonar pings were recorded and averaged to obtain a mean acoustic backscatter profile throughout the water column. The same ping rate for all frequencies was set between 8 and 20 Hz depending on fine SSC: higher concentration of fine particles allows to increase the ping rate due to stronger sound attenuation. Total absence of unwanted surface or bottom reflections in the recorded profiles was checked to adjust the ping rate. The boat was kept as stationary as possible using a GPS while recording each averaged profile for about 4 min. The transducers were located around 2.5 m upstream of the boat engine to avoid recording the backscatter of the bubbles generated by the engine. We often acquired measurements at various positions along the river transect. Typically, one to three mean backscatter profiles were measured at each experimental site. In some cases, the suspension was not homogeneous laterally throughout the river cross-section and fairly different profiles were obtained across various positions along a river transect.

At each experimental site, the background noise level was recorded by setting the ABS on listening mode (no pulse emission). This allowed to confirm that the boat engine acoustic noise has too low frequencies to have any impact on the sonar signal.

3.3. Suspended Sediment Measurements

At each position where a mean (time-averaged) backscatter profile was recorded, water samples were collected at various depths throughout the water column using a 2 L Niskin horizontal bottle sampler. The actual depth was measured using a pressure sensor attached to the sampler. The lowest water samples were taken at heights between 0.1 and 1.3 m above the riverbed. This sampler takes instantaneous samples and is not isokinetic (Dramais et al., 2018). The Niskin bottle was used here because it is cheaper, and easier and faster to use from a boat than heavier isokinetic samplers, such as a US-P6 for instance, which are deployed from a cableway or a bridge, usually. An additional near-surface water sample (about 20 cm below the surface) was also collected by hand, without using the Niskin bottle. Water sampling was performed right before or right after the recording of the mean backscatter profile.

As a non-negligible amount of sand particles was expected at experimental sites S3, S4, and S5, full water samples were wet sieved at 63 μm to separate sand and fine sediment fractions. The SSC and PSD of each fraction was measured separately. The SSC and PSD of water samples from other sites were measured without separating sand and fine sediment fractions. In these cases, subsampling was performed in the field right after sample collection by manually stirring the full sample in a bucket and quickly filling the subsamples. In spite of careful operation, this method is not as accurate as separating fine and sand fractions (Dramais et al., 2018) and may lead to underestimation of the sand mode in the PSD, particularly for samples collected near the riverbed.

Water sample SSC was obtained by filtering. The PSD was measured using a laser grain-sizer Cilas 1190 or Malvern Mastersizer 2000. Ultrasonic deflocculation was applied to samples prior to PSD laser-diffraction analysis, so the size of individual particles, rather than possible flocs or aggregates, was measured. No observations of flocs in situ or in samples are available at those sites. No in situ observation of air micro-bubbles was neither conducted.

Any macroscopic organic debris was removed from the samples by hand. Organic matter was not burned off before determining sediment concentration and size distributions. Based on monitoring data acquired by the Rhône Sediment Observatory (Thollet et al., 2018), we know that the suspended organic contents at the experimental sites of this study are generally low (<5% of the suspended sediment mass). Typically, the mean concentrations of particulate organic carbon observed in the Rhône at Jons (representative of sites S1–S2), in the Isère at Beaumont-Monteux (representative of sites S3–S5) and in the Rhône at Arles (representative of sites S6–S7) are

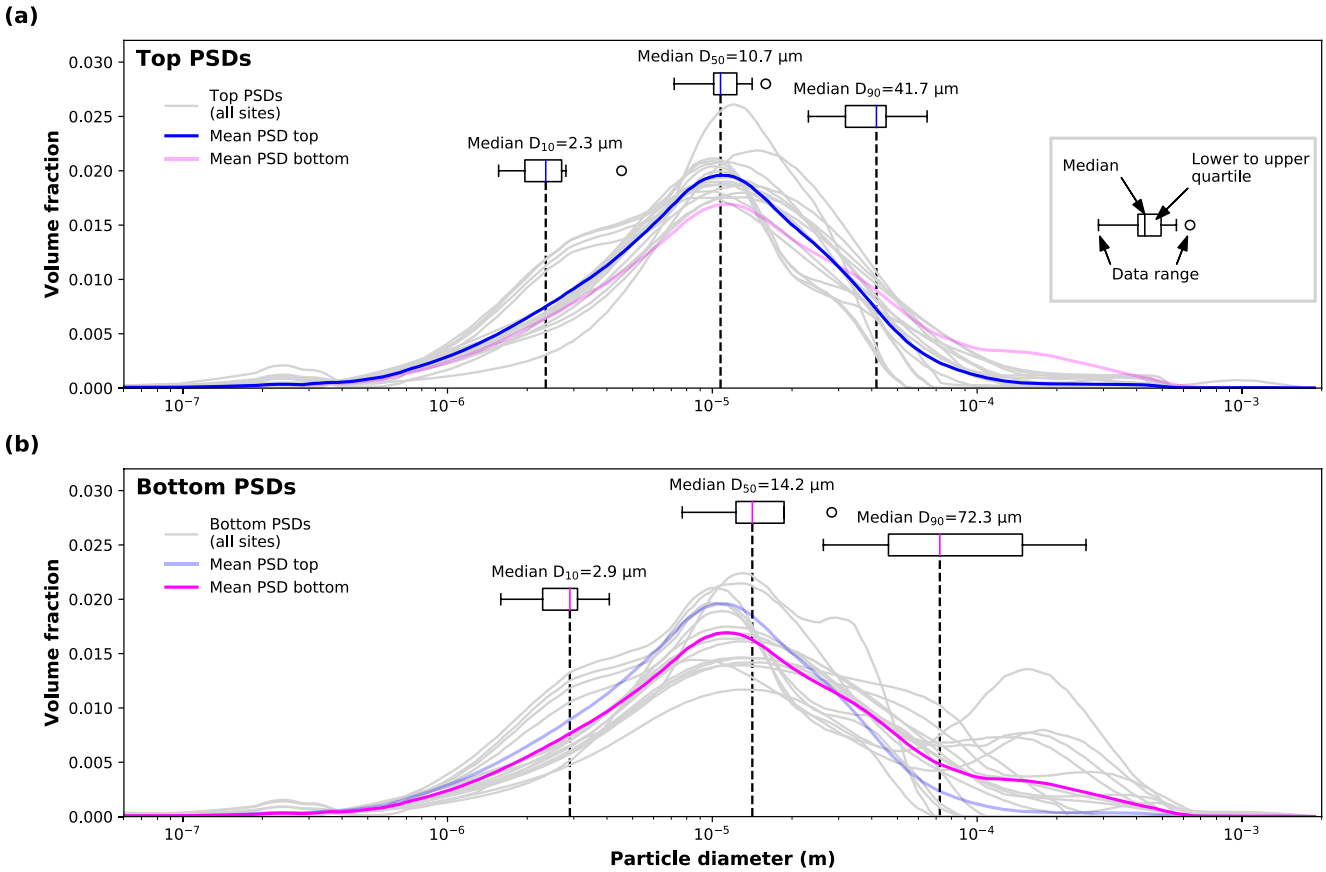

Figure 2. Volume Particle Size Distributions (PSDs) measured by laser diffraction for all samples collected (a) at the top of the water column; and (b) closest to the riverbed. Gray lines show all measured PSDs, colored lines show the mean PSD at the top and bottom of the water column, respectively, and boxplots show statistical information on D_{10}, D_{50}, and D_{90}, respectively.

32 g/kg (2011–2020, 211 samples), 18 g/kg (2014–2019, 35 samples), and 41 g/kg (2007–2019, 3,848 samples), respectively.

Details on PSD and SSC data used in this study are presented in Appendix B.

3.4. Particle Size Distributions

Laser diffraction measurements of the PSD are presented in Figure 2a for all the samples collected at the top of the water column (near-surface water samples collected by hand). Figure 2b presents the PSD measurements for the samples collected closest to the riverbed using the Niskin sampler. PSD statistics (D_{10}, D_{50}, D_{90}) for all the samples collected at all experimental sites are presented in Appendix B. As expected in rivers, the suspended particles observed in this study are a mixture of fines (clay and silt) and of fine sand particles covering a range of diameters of several orders of magnitude. Fines dominate the PSD and, whereas their concentration substantially vary, from 0.01 to 10 g/l approximately, their size remains relatively constant (around 10 µm) regardless of the experimental site, depth of sample collection or flow conditions.

As usually observed in rivers, the size distribution of the sand particles is much more variable. These particles are mainly found at the bottom of the water column, therefore samples collected close to the riverbed show higher and more variable D_{90} than samples collected close to the surface, as shown in Figure 2. The Rhône River bed is mainly made of gravel with deposits of sand and fine sediment locally.

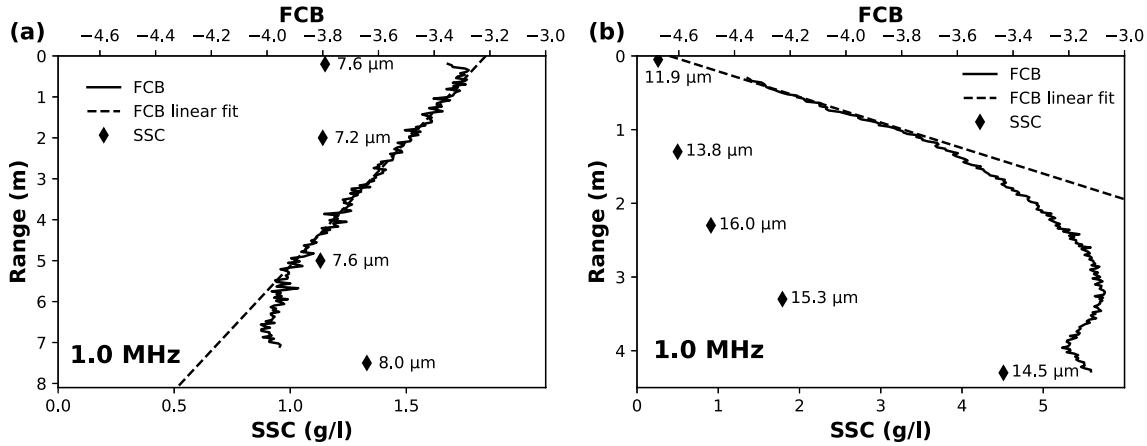

Figure 3. Examples of Fluid Corrected Backscatter profiles (FCB, solid lines) recorded at 1.0 MHz (a) at Site S6 with a homogeneous suspension at the top of the water column; (b) at Site S1 with a non-homogeneous suspension. Dashed lines show linear fits of the first cells of the FCB profiles, diamonds show measured suspended sediment concentration from water samples, along with the corresponding D_{50} measured by laser diffraction.

3.5. Mean Backscatter Profiles Modeling

Water sample PSD and SSC data were used to model the theoretical mean acoustic backscatter profiles. First, PSD and SSC data were interpolated in order to obtain a PSD and a value of SSC in each range cell of the sonar profile. SSC data were linearly interpolated throughout the water column. For PSD interpolation, the volume fraction of each size class was: (a) linearly interpolated between the various sample locations throughout the water column; and (b) normalized in order to make the sum of all fractions of the interpolated PSD at a given range from the transducer equal to one. The SSC and PSD are assumed constant between the deepest water sample and the riverbed. No extrapolation was needed at the top of the water column as near-surface water samples were collected very close to the transducers.

Interpolated SSC and PSD data were used to compute s_v, α_s, and $\overline{V^2}$ in each range cell of the sonar profile from Equations 1–3, respectively. The background noise level recorded at the experimental site was finally added to $\overline{V^2}$ to obtain a theoretical mean backscatter profile that can be compared with the recorded profile.

3.6. Near-Surface Backscatter and Attenuation Estimation

To get more information on the ability of the theory to model the sonar signal, it is usually necessary to deal with acoustic backscatter and acoustic attenuation separately. This implies to separate these two competing mechanisms in the analysis of the recorded sonar signal.

For the case of a homogeneous suspension, the extraction of α_s and s_v from the recorded mean backscatter profile has been usually done using the Fluid Corrected Backscatter (FCB, see e.g., Wright et al., 2010; Moore et al., 2012). The FCB can be derived from the sonar equation (Equation 1) as:

$$\begin{aligned} \mathrm{FCB} &= \frac{1}{2}\log_e\left(\overline{V^2} r^2 \mathrm{e}^{4r\alpha_w}\right) \\ &= \frac{1}{2}\log_e\left(\frac{16\pi k_t^2}{3} s_v(r)\right) - 2r\alpha_s(r) \end{aligned} \tag{7}$$

When the suspension is homogenous along the sonar beam, s_v and α_s are constant and the FCB varies linearly with range r. The values of s_v and α_s can be evaluated from the intercept and the slope of the FCB profile, respectively. This was done in the present study when the suspension was fairly homogeneous in the first meters of the water column, as illustrated in Figure 3a. Note that α_s cannot be estimated using this method when the slope of the FCB profile is too low, typically below 0.1, which corresponds to $\alpha_s = 0.05\ \mathrm{m}^{-1}$, because measurement errors become large compared to the slope value.

Even when the suspension is not homogeneous, it was observed at many experimental sites that the FCB often varies fairly linearly with range r in the first cells of the sonar profile after the transducer near field area (example in Figure 3b). Nevertheless α_s cannot be estimated from the FCB slope, as α_s and s_v certainly vary with range r. But as these variations lead to a linear variation of the FCB, it is possible to linearly extrapolate the FCB toward $r = 0$ as shown in Figure 3b. This linear extrapolation is supported by the fact that the FCB is well defined everywhere in the water column as it only depends on s_v, k_t, r, and α_s. Moreover, as the FCB depends directly on the properties of the suspension and is a logarithmic value, it is unlikely that abrupt variations can occur in the extrapolated part of the FCB profile toward the transducer. Abrupt variations of the FCB would imply abrupt variations in concentration and/or particle size, which near the surface is rather unlikely. At $r = 0$, that is the location of the transducer, the acoustic attenuation is null as there is no acoustic path but s_v is still defined and can be estimated from the intercept of the FCB linear fit:

$$s_v(r = 0) = \frac{3 \exp(2b)}{16\pi k_t^2} \tag{8}$$

where b is the intercept of the FCB linear fit, for example, $b = -4.6$ for the FCB profile presented in Figure 3b. This provides an estimation of s_v at the location of the transducer from the recorded sonar signal. As near-surface water samples were collected very close to the location of the transducers, it was possible to compare modeled values of α_s and s_v with "measured" values obtained from the FCB linear fit at the depth of the sampling location, around 20 cm below the surface.

We believe that such acoustic signal processing lead to parameter estimates with limited errors compared to the backscatter profile modeling errors which are explored in the next sections.

4. Results

4.1. Backscatter Profile Modeling

Figure 4 shows examples of modeled and recorded backscatter profiles at three different experimental sites. A similar trend is observed at all the other sites: the modeled acoustic backscatter signal is dramatically underestimated at low frequencies (≤1.0 MHz). Below 1.0 MHz, model errors can be as high as two orders of magnitude. Such a departure cannot be explained by calibration errors since the recorded backscatter profiles fall outside the envelope of simulated profiles (dashed lines) corresponding to a quite extreme variation of k_t of ±75% around the value given by the manufacturer. At frequencies higher than 1.0 MHz, model outputs and measurements are in better agreement. However, the modeled backscatter often decreases less rapidly with depth than the recorded profile (see for instance Figure 4b for frequencies 2.5 and 5.0 MHz and depths between 1 and 2 m). This probably indicates that acoustic attenuation was underestimated by the model. Note that the measured backscatter profiles shown in Figure 4 tend to become constant below a given depth at high frequency (>1.0 MHz). This is due to strong sound attenuation that makes the backscatter signal falling below the background noise level. This background noise level has been added to the modeled profiles.

4.2. Near-Surface Acoustic Backscatter and Attenuation

The "measured" values of s_v and α_s close to the surface (extracted from the sonar signal using the FCB technique described in Section 3.6) are compared with the modeled values (obtained using the near-surface PSD and SSC data) in Figure 5. Results presented in Figure 5a confirm what we observed in the backscatter profiles (Figure 4): modeled s_v values computed using the solid particle theory for the lowest frequencies are systematically underestimated. The absolute error can be as dramatic as two orders of magnitude at 0.3 and 0.5 MHz. Model outputs better agree with the measurements at 4.0 and 5.0 MHz. At all frequencies, the backscatter s_v clearly increases with SSC (see colors in Figure 5a), although at low frequency s_v values are very scattered.

Figure 5b compares modeled α_s with estimated values obtained from the FCB technique when a homogeneous suspension was found at the top of the water column. There are fewer points in Figure 5b compared with Figure 5a because α_s could not be estimated from acoustic measurement when the suspension was not homogeneous at the top of the water column or when α_s was too low, that is, at low frequency and very low SSC (cf. Section 3.6). At low frequency (0.3 and 0.5 MHz), modeled α_s values are particularly underestimated for concentrations lower

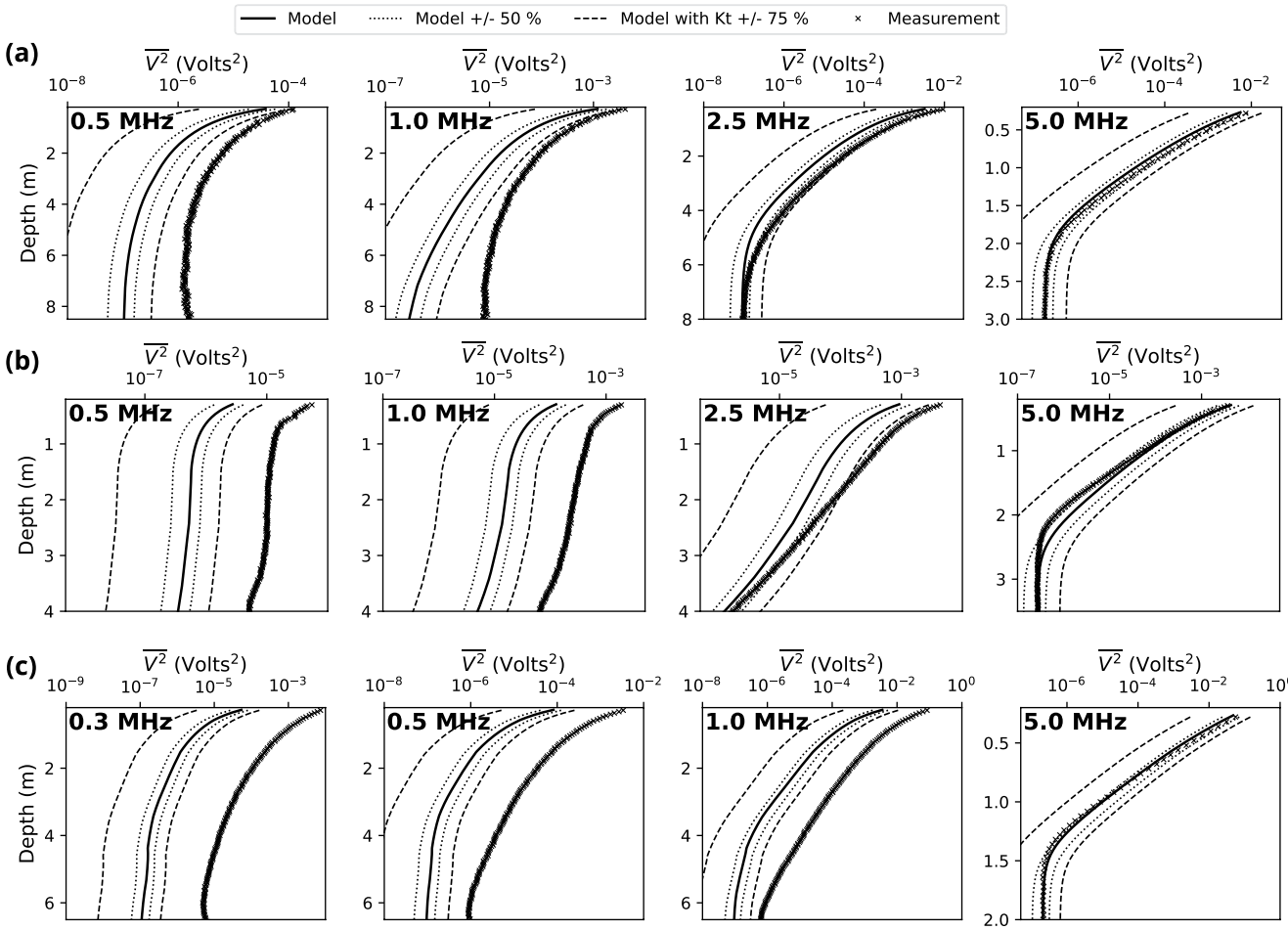

Figure 4. Examples of mean vertical backscatter profiles throughout the water column: (a) at Site S2, suspended sediment concentration (SSC) ~0.03 g/l; (b) at Site S1, SSC ~1 g/l; (c) at Site S7, SSC ~3 g/l. Solid lines show acoustic backscatter profile simulations, dotted lines show the ±50% band around the simulated profiles, dashed lines show the band around the simulated profiles corresponding to an error of ±75% on the instrument calibration constant k_t, crosses show the acoustic measurements.

than 1.0 g/l. The discrepancies between modeled and measured α_s tend to decrease when SSC increases. This is consistent with other observations made using side-looking ADCPs (Haught et al., 2017). At higher frequencies (4.0 and 5.0 MHz), modeled α_s values tend to be systematically underestimated, which is consistent with the less steep slopes of the modeled backscatter profiles observed in Figure 4.

4.3. Backscatter Echo Distribution

The various experimental backscatter echo distributions recorded in the Rhône River were compared with the theoretical Rayleigh distribution, with γ computed as $\gamma = \overline{V^2}$ (see Figure 6). Each plot of Figure 6 shows statistics of the raw signal recorded by the instrument in one sonar cell over many pings (typically 2000). Echo values were normalized by γ, following the method described in the Appendix B of Lee and Stanton (2014). All backscatter data were recorded with a signal to (background) noise ratio (SNR) higher than 10. Maximum recorded single echo value is 0.2005 V, far from saturation point estimated around 0.7 V. Three situations were often observed:

1. the recorded echo distributions at all frequencies acceptably follow Rayleigh distributions (Figure 6a);
2. a strong deviation from Rayleigh statistics is observed, most often at low frequency (Figure 6b) but sometimes at high frequency (Figure 6c);
3. a deviation from Rayleigh statistics is observed only in the "tail" of the distribution, that is, at the right end of the distribution (Figure 6d).

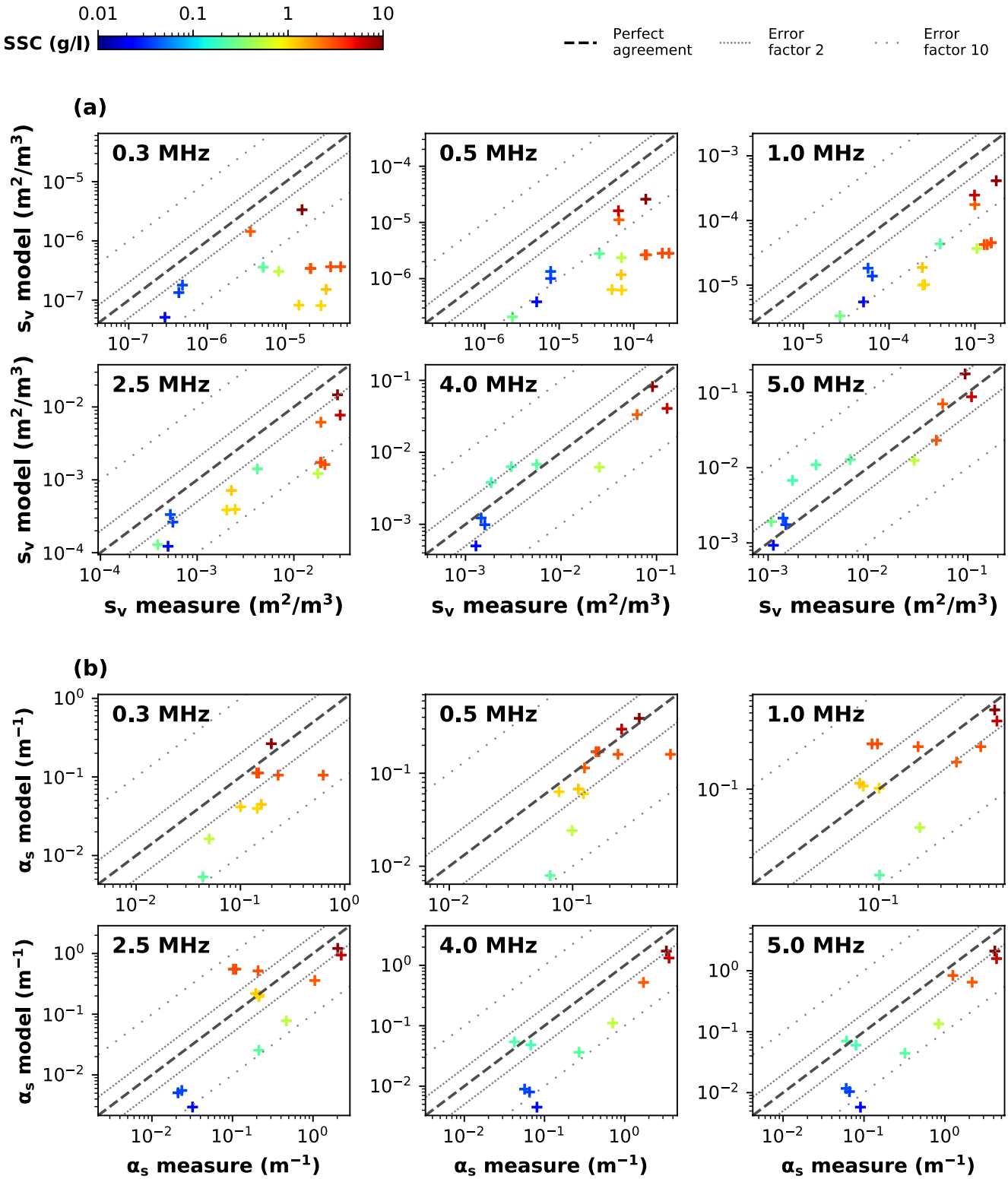

Figure 5. Model outputs versus acoustic measurements for near-surface water samples (a) volume backscattering s_v; (b) sediment attenuation α_s. Black dashed line is the line of perfect agreement, gray dotted lines indicate factor 2 and 10 differences.

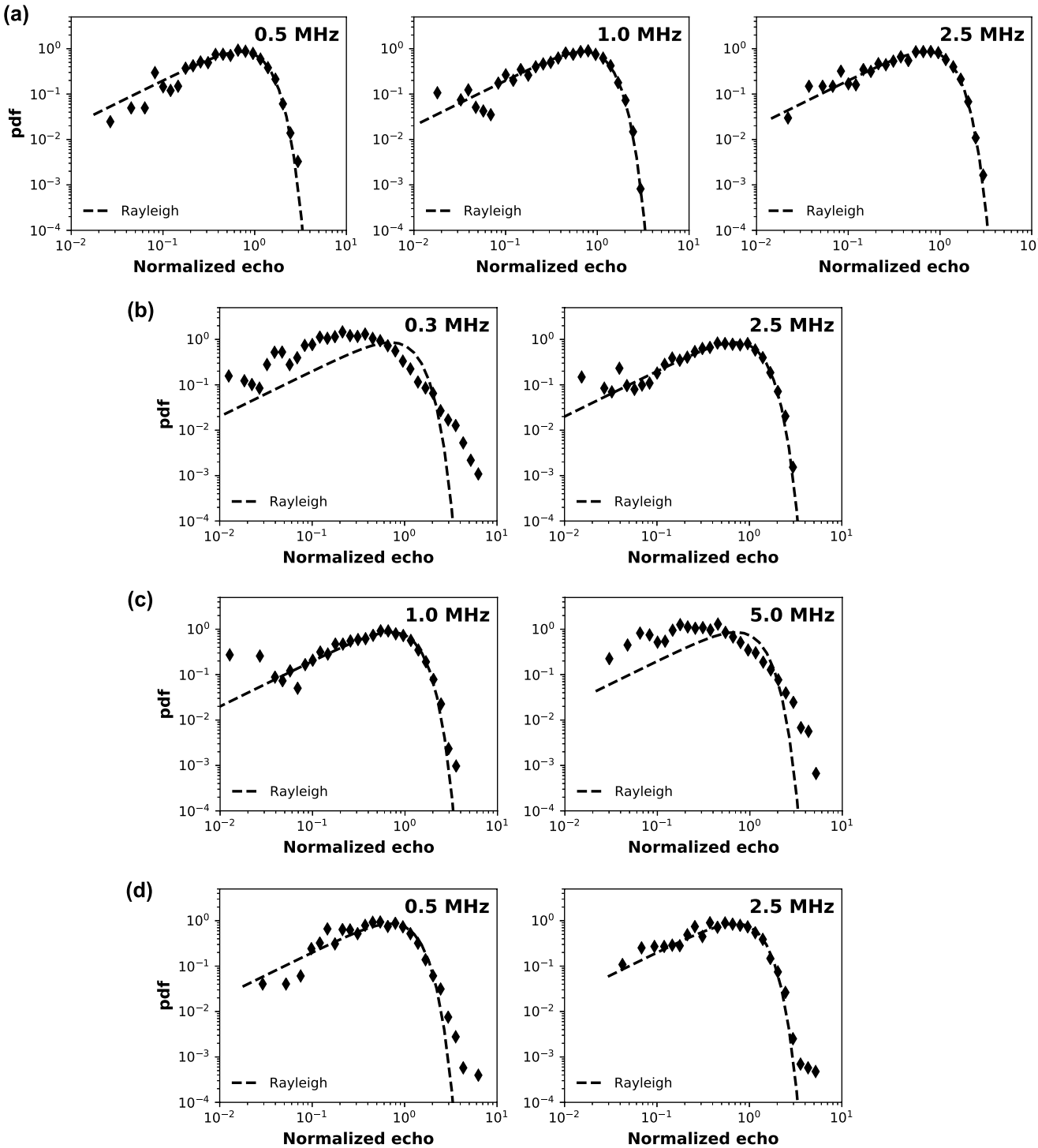

Figure 6. Backscatter echo distributions recorded: (a) at Site S1, 3.0 m depth; (b) at Site S6, 1.0 m depth; (c) at Site S4, 1.2 m depth; (d) at Site S6, 2.9 m depth. Dashed lines show the theoretical Rayleigh probability density function (pdf).

In our experiments, the first case (Figure 6a), that is, agreement with Rayleigh statistics, is not the most frequent. Generally, better agreement with Rayleigh statistics was observed at higher frequencies.

5. Discussion of Backscatter Modeling Errors

5.1. Ignored Types of Scatterers

The application of the solid particle theory to river suspensions may fail if other types of scatterers are present. Those other types of scatterers may include air micro-bubbles, flocs, organic particles, turbulent micro-structures and large scatterers (fish, plants, debris), as reviewed hereafter.

The presence of air micro-bubbles, potentially generated by a number of sources including wind waves, bank wake waves, weirs, obstacle backwash, cavitation or navigation could have a strong impact on both s_v and α_s (Ainslie & Leighton, 2011; Dalen & Løvik, 1981; Medwin & Clay, 1998; Richards & Leighton, 2001; Schat, 1997). Air micro-bubble target strength is particularly large around the bubble resonance frequency that is close to $0.0136 \times c/(2\pi a_b)$ with c the sound celerity and a_b the bubble radius (Medwin & Clay, 1998). As smaller bubbles tend to dissolve and larger ones tend to move toward the surface, the median radius of air micro-bubbles commonly lies in the range 10–100 μm. Then, the potential effect of air micro-bubbles is greater at low frequencies (<1.0 MHz), all the more that the target strength of suspended particles is smaller at these frequencies. On the contrary, the potential impact of air micro-bubbles on the recorded signal is expected to vanish at high frequencies (>1.0 MHz) as the ratio of air micro-bubble target strength to suspended sediments target strength decreases. This could potentially explain why measured s_v values are much greater than model predictions at low frequencies in Figure 5a, whereas better agreement is found at high frequencies.

Flocculation is a complex phenomenon that involves a number of physical, chemical, and biological processes (Droppo, 2001). Recent studies showed that flocculation can increase the level of backscatter (s_v) of a suspension of fine sediments (MacDonald et al., 2013; Rouhnia et al., 2014). The target strength of a floc is expected to be much smaller than the target strength of a solid particle with same size, but much greater than the target strength of the primary particles (Fromant et al., 2017; Sahin et al., 2017; Thorne et al., 2014; Vincent & MacDonald, 2015). When frequency increases, flocs reach the geometric scattering regime before primary particles so that the ratio of flocs target strength to primary particles target strength decreases. As opposed to the Rayleigh regime, the geometric regime happens when the particle size is large compared to the acoustic wavelength. Then, the target strength reaches a maximum and the form factor f_∞ does not depend on the size of the particles. Similar to air micro-bubbles, the effect of flocs on the recorded signal is expected to be greater at low frequencies (<1.0 MHz). This is another assumption for explaining s_v model/measurement discrepancies observed in Figure 5a.

At least two other known sources of sound scattering could potentially impact the recorded signal in rivers: micro-organisms (Stanton & Chu, 2000) and micro-structures generated by turbulence. The latter could be, in particular, temperature micro-gradients (Lavery et al., 2003, 2013; Ross & Lueck, 2003; Seim et al., 1995), or concentration micro-structures of micro-bubbles (Shen & Lemmin, 1997) or fine particles (Merckelbach, 2006). We could not investigate any of these processes due to the lack of observations.

5.2. Reasons for Non Rayleigh-Distributed Backscatter

As shown in Section 4.3, most of the recorded backscatter echo distributions deviate from the Rayleigh distribution expected from the usual assumptions behind the solid particle theory. Deviation from Rayleigh statistics may be due to large echoes from resolved scatterers, or to a small number of dominant unresolved scatterers, or to clusters of small scatterers. These possible explanations are discussed hereafter.

In the sonar theory, two scatterers are "resolved" if their target strengths are sufficiently strong and their distances to the transducer differ by more than half the emitted pulse length in water (Simmonds & MacLennan, 2005). Resolved scatterers produce separate echoes that can be clearly identified in the sonar profile (Chu & Stanton, 2010). In rivers, examples of resolved scatterers include fishes or small debris like leaves or branches. Conversely, individual echoes from suspended particles cannot be separated: these scatterers are unresolved. Resolved scatterers occasionally bring much larger echoes than the backscatter typically produced by the suspension. In terms of statistics, rare and strong echo values could lead to a deviation from the Rayleigh theory at the very right end of the distribution in a similar way as observed in Figure 6d. Even if they are rare, large echoes

from resolved scatterers can significantly increase the value of the Rayleigh estimator $\left(\gamma \approx \overline{V^2}\right)$ and lead to s_v overestimation. As large echo values result in signal "spikes," they would certainly be detected and removed using despiking algorithms as usually performed in preprocessing the acoustic signal (e.g., Vergne et al., 2020).

For a single type of particles (e.g., only sand particles of same size), the statistical distribution of the recorded amplitudes is a Rayleigh distribution if the number of particles in the sonar cell exceeds 20, approximately, according to Tuthill et al. (1988). When the number of scatterers is smaller, the resulting backscatter echo is no longer Rayleigh-distributed (Stanton & Clay, 1986). The obtained distribution is sometimes called "heavy-tailed": strong echoes are more probable than predicted by Rayleigh statistics. The same issue arises when the suspension is composed of scatterers of significantly different target strengths. Even if the total number of scatterers is large, echo statistics can diverge from Rayleigh if the number of dominant scatterers is too small (Lee & Stanton, 2014). This effect could be the source of some observed deviations from Rayleigh statistics (cf. Figure 6b). Even if they are much fewer than small particles, large solid particles, flocs and/or air micro-bubbles could potentially dominate the backscatter (s_v), at least at low frequencies (<1.0 MHz). Narrower sonar beam and/or smaller cell size may increase the "heavy tail" effect by reducing the ensonified volume (Chu & Stanton, 2010). For example, for a sediment density of 2,650 kg m^{-3} and a frequency of 0.5 MHz, the model of Thorne and Meral (2008) predicts that only 2.2×10^{-4} g/l of sand particles with radius $a = 100$ µm produce the same backscatter (s_v) as 0.5 g/l of fine sediments with radius $a = 7.5$ µm. For such a low concentration of sand, the number of sand particles in the ensonified volume at 1 m from the transducer used in this study would be around 5, considering a transducer diameter of 24 mm, a typical cell size of 2 cm, and an ensonified volume at −3 dB around the acoustic axis. This illustrates that a very small number of large scatterers can compete with relatively high concentrations of fine sediments in contributing to the sonar signal.

Strong deviations from Rayleigh statistics may be the most complicated problem to account for. When several different sources of sound backscattering are found, s_v is the sum of all these sources in the sonar equation (Equation 1) only if these sources all have Rayleigh-distributed echoes. If this condition is not met, the sonar equation might not be valid.

Turbulence is suspected to be able to "gather" small scatterers in turbulent structures, leading to clusters of scatterers. Then, the scatterers do not have a random position anymore and the backscatter signal is no longer incoherent. Clusters of scatterers may produce larger echoes than randomly-distributed scatterers, finally leading to a deviation of the backscatter echo distribution from Rayleigh statistics. Merckelbach (2006) argued that clusters of fine solid particles were the cause of the backscatter excess observed with a vertical ADCP in a tidal inlet. Shen and Lemmin (1997) showed that clusters of very small air bubbles could be the cause of the backscatter echoes recorded in laboratory facilities (flume and grid-stirred tank) in the absence of other scattering sources.

5.3. Errors Due To Particle Determination

Due to the field operation difficulties, the high spatio-temporal variability of the suspension and the sediment analysis uncertainty, especially when samples contain sand-sized particles (Dramais et al., 2018), the uncertainty of particle concentration and size may induce substantial errors in backscatter modeling. These errors are still difficult to estimate and more precise techniques and procedures are needed to minimize them. They are reviewed briefly hereafter.

The water sampling procedure necessarily induces errors in the determination of the concentration and size of the particles ensonified by the acoustic instrument. In rivers and especially for flood conditions, water samples are often difficult to take at precise locations and depths along the sonar beam. Using satellite navigation system for positioning and a pressure logger for depth determination is recommended. Anyway, water sampling cannot be done exactly at the same place and time as the acoustic records. As the flow is turbulent and the suspension varies with time, the temporal representativeness of instantaneous or integrated samples should be assessed. Quantifying the related uncertainties remains a challenge (e.g., Topping et al., 2011).

Large and difficult-to-estimate uncertainties could come out when measuring the PSD of fine sediments using laser diffraction (Eshel et al., 2004). In addition, the particle "radius" measured by laser diffraction is a rather ambiguous concept (Erdoğan et al., 2007) as also is the "radius" parameter used in acoustic modeling (Schaafsma & Hay, 1997). In practice, the radius or radius distribution of a suspension of natural sediments may differ

depending on the physical process that is considered (sedimentation, light scattering, acoustic scattering, acoustic attenuation due to viscous drag, etc.). This is particularly the case for fine suspended sediments that are usually highly non-spherical. This could potentially explain the underestimation of α_s by the model as observed in this study (Figure 5b) and in other studies (Haught et al., 2017; Vergne et al., 2021).

6. Conclusion

The objective of this study is to explore the possibilities and limitations of modeling sound backscattering by sediment suspensions in rivers using currently available theory. The main issues affecting the measurement of sediment suspension using an ABS are compiled and reviewed through a single experimental study, demonstrating that in some cases the solid particle theory is not well suited to the river suspensions. Some of the discussed issues were already published in various papers across diverse communities (ocean/river applications, acoustics/signal theory). However, the poor modeling of acoustic signal in rivers was never inspected in such a direct way, avoiding signal inversion errors and error compensation through field calibration. Especially, the statistical distribution of the acoustic signals measured in rivers was never analyzed whereas we found that the deviations from Rayleigh statistics may be closely related to errors in interpreting the acoustic backscatter signal recorded in rivers.

Using SSC and PSD data from water samples collected at various experimental sites of the Rhône River in France, we modeled the theoretical sonar signal using currently available backscatter and attenuation models. We compared this theoretical signal with the signal recorded in situ with a multifrequency ABS. A number of discrepancies were found. Close to the water surface, the modeled acoustic backscatter (s_v) was systematically underestimated for frequencies lower than 2.5 MHz. Model/measurement discrepancies increased when the frequency decreased. Errors could be as large as two orders of magnitude at 0.3 and 0.5 MHz, which cannot be explained by calibration errors. Acoustic attenuation (α_s) also tended to be underestimated by the models, particularly at low concentrations (<0.1 g/l). In some cases, the statistics of measured echoes showed strong deviations from the theoretically expected Rayleigh distribution.

The solid particle theory used for modeling the sonar signal is based on the assumptions that acoustic backscattering is due to a sufficient number of similar non-cohesive particles in the ensonified volume, made of solid material and having random positions. This theory was originally developed in acoustical oceanography for monitoring sand suspensions. The discrepancies between model and measurements observed in this study could be due to deviations from these assumptions in river environment. While the data collected in this study are insufficient to identify the causes of observed model/measurement discrepancies, several error sources were discussed. Other sources of backscatter and attenuation could play a role in the recorded signal, including air micro-bubbles, flocs and organic particles. Turbulence could also increase the level of recorded backscatter by setting up either temperature micro-gradients and/or clusters of scatterers. The accuracy of acoustic models in representing fine sediment effects could eventually be questioned, in particular regarding viscous attenuation. The non-isokinetic water sampling technique used in this study as well as the difficulty of measuring fine sediment PSD could also bring major sources of uncertainties in acoustic modeling. Deviations from the expected Rayleigh distribution could be due to the presence of resolved scatterers, or a small number of dominant unresolved scatterers, or turbulence-driven clusters of small scatterers. These effects could lead to heavy-tailed echo distributions and finally result in s_v overestimation when the Rayleigh estimator is computed as $\gamma \approx \overline{V^2}$. When several different sources of backscattering significantly contribute to the recorded signal, strong deviations from Rayleigh statistics could even challenge the validity of the generally used sonar equation.

The potential impact of all these processes in rivers is still unclear. Hopefully, some of them might be negligible in the usual conditions. Further work is needed to clarify which of these processes are significant and which ones can be neglected. Whereas severe limitations may arise, the solid particle theory can still be applied in rivers when the backscatter is dominated by a sufficient number of solid particles (typically sand). As shown in this study, better agreement with the theory will be more likely to happen at higher frequency and/or higher level of SSC.

Many research topics seem promising to enhance the understanding and modeling of the backscatter signal in rivers in order to improve inversion techniques. Efforts could be made to improve fine sediments acoustic modeling, in particular regarding viscous attenuation. Using the theoretical oblate spheroid model proposed by Richards et al. (2003) instead of the classical spherical model described in Urick (1948)—that has been used

in this study as well as in many others—is promising (Moore et al., 2013; Vergne et al., 2021). Developing semi-empirical backscatter and attenuation models as it has been done in marine science for sand particles would certainly greatly improve the representation of the crucial effect of fine sediments. Being able to separate acoustic backscatter and acoustic attenuation from the recorded signal in rivers is also a great source of information on acoustic processes. This can be achieved in rivers through several means, including horizontal deployment or use of targets of known backscatter such as a tungsten carbide sphere (Foote & Martini, 2010; Hwang et al., 2007) or riverbed echo previously recorded in clear water conditions (Thorne et al., 1995). Exploring the frequency backscatter response of the water column using a larger set of single frequency sonars (but not just a few uncalibrated ADCPs) or broadband sonars following the techniques under development in oceanography (e.g., Stanton et al., 2010) is another very promising field of research to potentially identify and separate different sources of backscatter like flocs or air micro-bubbles. Developments in oceanography also showed that exploring the sonar signal statistics could bring meaningful information on the backscatter sources (e.g., Lee & Stanton, 2016).

In any case, this work illustrates that even when applying a more rigorous method than generally applied in river studies (using ADCPs), significant errors exist and therefore it is not straightforward to invert the acoustic signal in order to estimate the SSC. There are already ways to go further (and other experiments to conduct) in the understanding of river suspension backscattering. With some efforts, it seems possible to develop a more complete theory suitable for interpreting river backscattering or, at least, to define the area of validity of the existing solid particle theory in terms of frequency, SSC, PSD, etc. This is necessary to increase the accuracy and robustness of hydroacoustic calibration methods as well as inversion methods for river applications.

The complexity and limitations of the acoustic backscatter technique applied to river sediment studies may seem discouraging to many practitioners. Indeed, this study suggests that the technique still requires more research and development than may be reflected in some published field calibration studies. However, the very high spatial and temporal resolution offered by the acoustic backscatter technique remains promising for a better understanding of suspended sediment (especially sand) processes in rivers. We wish that this paper enhance the link between river sediment applications using acoustic backscatter measurements and more theoretical research addressing the barriers that still impede the accurate and efficient deployment of this promising technology.

Appendix A: Instrument Calibration Data

The instrument calibration data (cf. Table A1) used in this study are determined by the manufacturer from the measurement of a suspension of glass beads. For each emitting frequency, values of the transducer constants k_t are given for the calibration set up: pulse length of 13.33 μs, sound celerity of 1,475 m/s and standard amplification (0 dB) for the emitted and received signal.

Table A1
Transducer Constants k_t of the Acoustic Backscatter System Used in This Study

Frequency (MHz)	k_t (V m$^{3/2}$)
0.3	0.04
0.5	0.01838
1.0	0.03267
2.5	0.01598
4.0	0.01538
5.0	0.01376

Appendix B: Summary of Water Sample Data

Table B1 provides the location, depth, mass concentration and volume particle size distribution statistics of all the water samples used in this study.

Table B1
Summary of Water Sample Data

Experimental site reference and coordinates	Position/flow depth[a] (m)	Sample depth[b] (m)	SSC (g/l)	D_{10} (μm)	D_{50} (μm)	D_{90} (μm)
S1 (45°39′11.05″N, 5°41′14.83″E)	138/4.6	0.2	0.26	2.7	11.9	29.2
		1.5	0.50	2.8	13.8	39.4
		2.5	0.91	3.4	16.0	43.6
		3.5	1.79	3.1	15.3	43.6
		4.5	4.51	2.9	14.5	39.4
S2 (45°43′33.39″N, 4°49′8.06″E)	20/8.8	1.0	0.03	2.7	14.1	61.3
		5.0	0.04	2.7	13.8	56.9
		7.5	0.04	2.4	12.9	58.0
	70/8.4	0.2	0.03	2.6	13.5	61.3
		4.0	0.04	3.1	16.4	87.4
		7.0	0.05	2.9	14.9	62.1
		8.0	0.04	2.6	14.1	79.9
	210/10.1	0.2	0.03	4.5	15.9	52.9
		2.0	0.02	3.9	13.8	46.7
		5.0	0.02	4.2	15.2	60.4
		9.0	0.02	4.0	14.1	53.3
S3 (44°59′39.06″N, 4°52′10.30″E)	110/4.4 (T1[c])	0.2	9.35	2.7	12.3	42.8
		3.1	12.81	3.1	16.3	85.3
		4.2	13.05	3.1	16.3	85.3
	100/4.0 (T2[c])	0.2	2.78	2.7	10.7	32.4
		0.7	6.37	2.7	14.2	64.7
		1.7	7.56	3.1	16.3	85.3
		3.3	8.72	3.1	18.7	85.3
S4 (44°59′5.18″N, 4°51′43.88″E)	55/11.4	0.2	0.24	2.4	11.4	40.6
		4.2	1.31	2.5	11.8	42.9
		8.5	1.26	2.7	14.2	85.3
		10.7	9.00	3.1	18.7	148.3
	95/11.2	0.2	0.55	2.3	10.7	42.8
		4.3	2.09	2.7	12.3	42.8
		7.2	3.80	2.3	10.7	37.2
		10.3	9.86	4.1	28.3	257.7
	150/8.4	0.2	0.53	2.3	10.7	42.8
		4.0	8.06	2.7	12.3	56.4
		6.8	13.00	2.3	12.3	224.4
		7.4	12.15	3.1	18.7	170.2
S5 (44°59′24.26″N, 4°52′1.88″E)	35/2.4	0.2	6.54	2.3	10.7	37.2
		1.0	13.11	2.7	14.2	56.4
		2.0	14.39	2.7	14.2	64.7

Table B1
Continued

Experimental site reference and coordinates	Position/flow depth[a] (m)	Sample depth[b] (m)	SSC (g/l)	D_{10} (μm)	D_{50} (μm)	D_{90} (μm)
	70/7.7	0.2	0.20	2.0	10.7	42.8
		4.0	0.43	3.6	24.6	129.1
		6.8	13.51	2.7	14.2	56.4
		7.3	16.96	3.1	18.7	148.3
	170/9.1	0.2	0.22	2.3	10.7	64.7
		4.3	0.33	2.3	12.3	112.5
		7.1	0.28	2.3	12.3	170.2
		7.8	0.28	2.3	14.2	224.4
S6 (43°24′55.89″N, 4°44′55.91″E)	100/10.2	0.2	1.28	1.8	8.0	29.2
		5.0	1.29	1.9	8.8	30.7
		8.0	1.35	1.7	8.4	32.3
		10.0	1.53	1.8	8.8	34.0
	290/8.7	0.2	1.15	1.8	7.6	23.9
		2.0	1.14	1.5	7.2	23.9
		5.0	1.13	1.7	7.6	25.2
		7.5	1.33	1.8	8.0	27.8
	350/8.2	0.2	1.11	1.6	7.6	23.9
		3.0	1.17	1.6	8.0	27.8
		6.0	1.20	1.5	8.0	27.8
		8.0	1.40	1.7	8.4	32.3
S7 (43°23′20.01″N, 4°47′47.69″E)	40/6.7	0.1	3.10	1.6	8.4	30.7
		0.6	3.06	1.7	8.4	29.2
		1.6	3.19	1.7	8.8	32.3
		2.6	3.04	1.8	9.3	35.7
		3.6	3.35	1.8	9.3	35.7
		4.6	3.48	1.7	9.3	39.4
		5.6	4.06	2.0	10.2	45.8

[a]Position along the river transect, given as the distance from the left bank, of the point where acoustic measurements and water sampling were performed, and flow depth at this point. [b]Depth of water sample collection. [c]Data at S3 experimental site were collected in the Isère River at two different transects T1 and T2, located at 200 and 300 m from the confluence with the Rhône River, respectively.

Acknowledgments
Dan Hanes and two anonymous reviewers are gratefully acknowledged for their insightful comments on earlier versions of this manuscript. Adrien Vergne's PhD was partly funded by the Compagnie Nationale du Rhône (CNR 4200082173). Particle size laser-diffraction measurements were partly made at the Ecole Nationale des Travaux Publics de l'Etat (ENTPE). This study contributes to the Rhône Sediment Observatory (OSR), a multi-partner research program funded through the Plan Rhône by the European Regional Development Fund (ERDF), Agence de l'eau RMC, CNR, EDF and three regional councils of France (Auvergne-Rhône-Alpes, PACA and Occitanie).

Data Availability Statement

The data sets and the processing algorithms used in this study are archived in the following permanent repository: https://doi.org/10.57745/SGADUP (Vergne et al., 2023).

References

Agrawal, Y. C., & Hanes, D. M. (2015). The implications of laser-diffraction measurements of sediment size distributions in a river to the potential use of acoustic backscatter for sediment measurements. *Water Resources Research*, *51*(11), 8854–8867. https://doi.org/10.1002/2015wr017268

Ainslie, M. A., & Leighton, T. G. (2011). Review of scattering and extinction cross-sections, damping factors, and resonance frequencies of a spherical gas bubble. *Journal of the Acoustical Society of America*, *130*(5), 3184–3208. https://doi.org/10.1121/1.3628321

Armijos, E., Crave, A., Espinoza, R., Fraizy, P., Dos Santos, A. L. M. R., Sampaio, F., et al. (2017). Measuring and modeling vertical gradients in suspended sediments in the Solimões/Amazon River. *Hydrological Processes*, *31*(3), 654–667. https://doi.org/10.1002/hyp.11059

Baranya, S., & Józsa, J. (2013). Estimation of suspended sediment concentrations with ADCP in Danube River. *Journal of Hydrology and Hydromechanics*, *61*(3), 232–240. https://doi.org/10.2478/johh-2013-0030

Betteridge, K. F. E., Thorne, P. D., & Cook, R. D. (2008). Calibrating multi-frequency acoustic backscatter systems for studying near-bed suspended sediment transport processes. *Continental Shelf Research*, *28*(2), 227–235. https://doi.org/10.1016/j.csr.2007.07.007

Chu, D., & Stanton, T. K. (2010). Statistics of echoes from a directional sonar beam insonifying finite numbers of single scatterers and patches of scatterers. *IEEE Journal of Oceanic Engineering*, *35*(2), 267–277. https://doi.org/10.1109/joe.2009.2037988

Dalen, J., & Løvik, A. (1981). The influence of wind-induced bubbles on echo integration surveys. *Journal of the Acoustical Society of America*, *69*(6), 1653–1659. https://doi.org/10.1121/1.385943

Downing, A., Thorne, P. D., & Vincent, C. E. (1995). Backscattering from a suspension in the near field of a piston transducer. *Journal of the Acoustical Society of America*, *97*(3), 1614–1620. https://doi.org/10.1121/1.412100

Dramais, G., Camenen, B., Le Coz, J., Thollet, F., Le Bescond, C., Lagouy, M., et al. (2018). Comparison of standardized methods for suspended solid concentration measurements in river samples. In *Proceedings of the river flow 2018 conference* (Vol. 40). https://doi.org/10.1051/e3sconf/20184004018

Droppo, I. G. (2001). Rethinking what constitutes suspended sediment. *Hydrological Processes*, *15*(9), 1551–1564. https://doi.org/10.1002/hyp.228

Erdoğan, S., Garboczi, E. J., & Fowler, D. (2007). Shape and size of microfine aggregates: X-Ray microcomputed tomography vs. laser diffraction. *Powder Technology*, *177*(2), 53–63. https://doi.org/10.1016/j.powtec.2007.02.016

Eshel, G., Levy, G. J., Mingelgrin, U., & Singer, M. J. (2004). Critical evaluation of the use of laser diffraction for particle-size distribution analysis. *Soil Science Society of America Journal*, *68*(3), 763–743. https://doi.org/10.2136/sssaj2004.7360

Foote, K. G., & Martini, M. A. (2010). Standard-target calibration of an acoustic backscatter system. In *Oceans 2010 MTS/IEEE Seattle* (pp. 1–5). https://doi.org/10.1109/OCEANS.2010.5664362

François, R. E., & Garrison, G. R. (1982). Sound absorption based on ocean measurements: Part I: Pure water and magnesium sulfate contributions. *Journal of the Acoustical Society of America*, *75*(3), 896–907. https://doi.org/10.1121/1.388170

Fromant, G., Floc'h, F., Lebourges-Dhaussy, A., Jourdin, F., Perrot, Y., Le Dantec, N., & Delacourt, C. (2017). In situ quantification of the suspended load of estuarine aggregates from multifrequency acoustic inversions. *Journal of Atmospheric and Oceanic Technology*, *34*(8), 1625–1643. https://doi.org/10.1175/jtech-d-16-0079.1

Grams, P. E., Buscombe, D., Topping, D. J., Kaplinski, M., & Hazel, J. E. (2018). How many measurements are required to construct an accurate sand budget in a large river? Insights from analyses of signal and noise. *Earth Surface Processes and Landforms*, *44*(1), 160–178. https://doi.org/10.1002/esp.4489

Gray, J. R., & Landers, M. N. (2014). 1.10—Measuring suspended sediment. In *Comprehensive water quality and purification* (pp. 157–204). Elsevier. https://doi.org/10.1016/B978-0-12-382182-9.00012-8

Hanes, D. M. (2012). On the possibility of single-frequency acoustic measurement of sand and clay concentrations in uniform suspensions. *Continental Shelf Research*, *46*, 64–66. https://doi.org/10.1016/j.csr.2011.10.008

Hanes, D. M., Vincent, C. E., Huntley, D. A., & Clarke, T. L. (1988). Acoustic measurements of suspended sand concentration in the C2S2 experiment at Stanhope Lane, Prince Edward Island. *Marine Geology*, *81*(1–4), 185–196. https://doi.org/10.1016/0025-3227(88)90025-4

Haught, D., Venditti, J. G., & Wright, S. A. (2017). Calculation of in situ acoustic sediment attenuation using off-the-shelf horizontal ADCPs in low concentration settings. *Water Resources Research*, *53*(6), 5017–5037. https://doi.org/10.1002/2016wr019695

Hay, A. E. (1983). On the acoustic detection of suspended sediment at long wavelengths. *Journal of Geophysical Research*, *88*(C12), 7525–7542. https://doi.org/10.1029/jc088ic12p07525

Hay, A. E. (1991). Sound scattering from a particle-laden, turbulent jet. *Journal of the Acoustical Society of America*, *90*(4), 2055–2074. https://doi.org/10.1121/1.401633

Hay, A. E., & Sheng, J. (1992). Vertical profiles of suspended sand concentration and size from multifrequency acoustic backscatter. *Journal of Geophysical Research*, *97*(C10), 15661–15677. https://doi.org/10.1029/92jc01240

Holdaway, G. P., Thorne, P. D., Flatt, D., Jones, S. E., & Prandle, D. (1999). Comparison between ADCP and transmissometer measurements of suspended sediment concentration. *Continental Shelf Research*, *19*(3), 421–441. https://doi.org/10.1016/s0278-4343(98)00097-1

Hwang, B. K., Furusawa, M., & Ogata, M. (2007). Validation of multi-frequency inversion method by using dummy scatterers of zooplankton. *Fisheries Science*, *73*(2), 250–262. https://doi.org/10.1111/j.1444-2906.2007.01331.x

Landers, M. N., Straub, T. D., Wood, M. S., & Domanski, M. M. (2016). Sediment acoustic index method for computing continuous suspended-sediment concentrations. In *USGS Techniques and Methods, Book 3, Chapter C5*. https://doi.org/10.3133/tm3C5

Latosinski, F. G., Szupiany, R. N., García, C. M., Guerrero, M., & Amsler, M. L. (2014). Estimation of concentration and load of suspended bed sediment in a large river by means of acoustic doppler technology. *Journal of Hydraulic Engineering*, *140*(7), 04014023. https://doi.org/10.1061/(asce)hy.1943-7900.0000859

Lavery, A. C., Geyer, W. R., & Scully, M. E. (2013). Broadband acoustic quantification of stratified turbulence. *Journal of the Acoustical Society of America*, *134*(1), 40–54. https://doi.org/10.1121/1.4807780

Lavery, A. C., Schmitt, R. W., & Stanton, T. K. (2003). High-frequency acoustic scattering from turbulent oceanic microstructure: The importance of density fluctuations. *Journal of the Acoustical Society of America*, *114*(5), 2685–2698. https://doi.org/10.1121/1.1614258

Lee, W.-J., & Stanton, T. K. (2014). Statistics of echoes from mixed assemblages of scatterers with different scattering amplitudes and numerical densities. *IEEE Journal of Oceanic Engineering*, *39*(4), 740–754. https://doi.org/10.1109/joe.2013.2285657

Lee, W.-J., & Stanton, T. K. (2016). Statistics of broadband echoes: Application to acoustic estimates of numerical density of fish. *IEEE Journal of Oceanic Engineering*, *41*(3), 709–723. https://doi.org/10.1109/joe.2015.2476619

Libicki, C., Bedford, K. W., & Lynch, J. F. (1989). The interpretation and evaluation of a 3-MHz acoustic backscatter device for measuring benthic boundary layer sediment dynamics. *Journal of the Acoustical Society of America*, *85*(4), 1501–1511. https://doi.org/10.1121/1.397351

MacDonald, I. T., Vincent, C. E., Thorne, P. D., & Moate, B. D. (2013). Acoustic scattering from a suspension of flocculated sediments. *Journal of Geophysical Research*, *118*(5), 2581–2594. https://doi.org/10.1002/jgrc.20197

Medwin, H., & Clay, C. S. (1998). *Fundamentals of acoustical oceanography*. Academic Press.

Merckelbach, L. M. (2006). A model for high-frequency acoustic Doppler current profiler backscatter from suspended sediment in strong currents. *Continental Shelf Research*, *26*(11), 1316–1335. https://doi.org/10.1016/j.csr.2006.04.009

Moate, B. D., & Thorne, P. D. (2012). Interpreting acoustic backscatter from suspended sediments of different and mixed mineralogical composition. *Continental Shelf Research*, *46*, 67–82. https://doi.org/10.1016/j.csr.2011.10.007

Moate, B. D., Thorne, P. D., & Cook, R. D. (2016). Field deployment and evaluation of a prototype autonomous two dimensional acoustic backscatter instrument: The Bedform and Suspended Sediment Imager (BASSI). *Continental Shelf Research*, *112*, 78–91. https://doi.org/10.1016/j.csr.2015.10.017

Moore, S. A., Le Coz, J., Hurther, D., & Paquier, A. (2012). On the application of horizontal ADCPs to suspended sediment transport surveys in rivers. *Continental Shelf Research*, *46*, 50–63. https://doi.org/10.1016/j.csr.2011.10.013

Moore, S. A., Le Coz, J., Paquier, A., & Hurther, D. (2013). Using multi-frequency acoustic attenuation to monitor grain size and concentration of suspended sediment in rivers. *Journal of the Acoustical Society of America*, *133*(4), 1959–1970. https://doi.org/10.1121/1.4792645

Reichel, G., & Nachtnebel, H. P. (1994). Suspended sediment monitoring in a fluvial environment: Advantages and limitations applying an acoustic Doppler current profiler. *Water Research*, *28*(4), 751–761. https://doi.org/10.1016/0043-1354(94)90083-3
Richards, S. D., & Leighton, T. G. (2001). Acoustic sensor performance in coastal waters: Solid suspensions and bubbles. In *Acoustical oceanography, proceedings of the institute of acoustics* (Vol. 23, pp. 399–406).
Richards, S. D., Leighton, T. G., & Brown, N. R. (2003). Visco-inertial absorption in dilute suspensions of irregular particles. *Proceedings of the Royal Society of London*, *459*(2037), 2153–2167. https://doi.org/10.1098/rspa.2003.1126
Ross, T., & Lueck, R. (2003). Sound scattering from oceanic turbulence. *Geophysical Research Letters*, *30*(6), 1343–1346. https://doi.org/10.1029/2002gl016733
Rouhnia, M., Keyvani, A., & Strom, K. (2014). Do changes in the size of mud flocs affect the acoustic backscatter values recorded by a Vector ADV? *Continental Shelf Research*, *84*, 84–92. https://doi.org/10.1016/j.csr.2014.05.015
Sahin, C., Verney, R., Sheremet, A., & Voulgaris, G. (2017). Acoustic backscatter by suspended cohesive sediments: Field observations, Seine Estuary, France. *Continental Shelf Research*, *134*, 39–51. https://doi.org/10.1016/j.csr.2017.01.003
Sassi, M. G., Hoitink, A. J. F., & Vermeulen, B. (2012). Impact of sound attenuation by suspended sediment on ADCP backscatter calibrations. *Water Resources Research*, *48*(9), W09520. https://doi.org/10.1029/2012wr012008
Sassi, M. G., Hoitink, A. J. F., Vermeulen, B., & Hidayat, H. (2013). Sediment discharge division at two tidally influenced river bifurcations. *Water Resources Research*, *49*(4), 2119–2134. https://doi.org/10.1002/wrcr.20216
Schaafsma, A. S., & Hay, A. E. (1997). Attenuation in suspensions of irregularly shaped sediment particles: A two-parameter equivalent spherical scatter model. *Journal of the Acoustical Society of America*, *102*(3), 1485–1502. https://doi.org/10.1121/1.420063
Schat, J. (1997). Multifrequency acoustic measurement of concentration and grain size of suspended sand in water. *Journal of the Acoustical Society of America*, *101*(1), 209–217. https://doi.org/10.1121/1.418003
Seim, H. E., Gregg, M. C., & Miyamoto, R. T. (1995). Acoustic backscatter from turbulent microstructure. *Journal of Atmospheric and Oceanic Technology*, *12*(2), 367–380. https://doi.org/10.1175/1520-0426(1995)012<0367:abftm>2.0.co;2
Shen, C., & Lemmin, U. (1997). Ultrasonic scattering in highly turbulent clear water flow. *Ultrasonics*, *35*(1), 57–64. https://doi.org/10.1016/s0041-624x(96)00091-1
Sheng, J., & Hay, A. E. (1988). An examination of the spherical scatterer approximation in aquaeous suspensions of sand. *Journal of the Acoustical Society of America*, *83*(2), 598–610. https://doi.org/10.1121/1.396153
Siddiqui, M. M. (1962). Some problems connected with Rayleigh distributions. *Journal of Research of the National Bureau of Standards*, *66D*(2), 167–174. https://doi.org/10.6028/jres.066d.020
Simmonds, J., & MacLennan, D. (2005). Fisheries acoustics (2nd ed.).
Stanton, T. K., & Chu, D. (2000). Review and recommendations for the modelling of acoustic scattering by fluid-like elongated zooplankton: Euphausiids and copepods. *ICES Journal of Marine Science*, *57*(4), 793–807. https://doi.org/10.1006/jmsc.1999.0517
Stanton, T. K., Chu, D., Jech, J. M., & Irish, J. D. (2010). New broadband methods for resonance classification and high-resolution imagery of fish with swimbladders using a modified commercial broadband echosounder. *ICES Journal of Marine Science*, *67*(2), 365–378. https://doi.org/10.1093/icesjms/fsp262
Stanton, T. K., & Clay, C. S. (1986). Sonar echo statistics as a remote-sensing tool: Volume and seafloor. *IEEE Journal of Oceanic Engineering*, *11*(1), 79–95. https://doi.org/10.1109/joe.1986.1145139
Szupiany, R. N., Weibel, C. L., Guerrero, M., Latosinski, F., Wood, M., Ruben, L. D., & Oberg, K. (2019). Estimating sand concentrations using ADCP-based acoustic inversion in a large fluvial system characterized by bi-modal suspended-sediment distributions. *Earth Surface Processes and Landforms*, *44*(6), 1295–1308. https://doi.org/10.1002/esp.4572
Thollet, F., Le Bescond, C., Lagouy, M., Gruat, A., Grisot, G., Le Coz, J., et al. (2018). Observatoire des Sédiments du Rhône. https://doi.org/10.17180/OBS.OSR
Thorne, P. D., & Buckingham, M. J. (2004). Measurements of scattering by suspensions of irregularly shaped sand particles and comparison with a single parameter modified sphere model. *Journal of the Acoustical Society of America*, *116*(5), 2876–2889. https://doi.org/10.1121/1.1808458
Thorne, P. D., & Campbell, S. C. (1992). Backscattering by a suspension of spheres. *Journal of the Acoustical Society of America*, *92*(2), 978–986. https://doi.org/10.1121/1.403967
Thorne, P. D., & Hanes, D. M. (2002). A review of acoustic measurement of small-scale sediment processes. *Continental Shelf Research*, *22*(4), 603–632. https://doi.org/10.1016/s0278-4343(01)00101-7
Thorne, P. D., & Hardcastle, P. J. (1997). Acoustic measurements of suspended sediments in turbulent currents and comparison with in-situ samples. *Journal of the Acoustical Society of America*, *101*(5), 2603–2614. https://doi.org/10.1121/1.418501
Thorne, P. D., Hardcastle, P. J., & Soulsby, R. L. (1993). Analysis of acoustic measurements of suspended sediments. *Journal of Geophysical Research*, *98*(C1), 899–910. https://doi.org/10.1029/92jc01855
Thorne, P. D., Holdaway, G. P., & Hardcastle, P. J. (1995). Constraining acoustic backscatter estimates of suspended sediment concentration profiles using the bed echo. *Journal of the Acoustical Society of America*, *98*(4), 2280–2288. https://doi.org/10.1121/1.413342
Thorne, P. D., & Hurther, D. (2014). An overview on the use of backscattered sound for measuring suspended particle size and concentration profiles in non-cohesive inorganic sediment transport studies. *Continental Shelf Research*, *73*, 97–118. https://doi.org/10.1016/j.csr.2013.10.017
Thorne, P. D., MacDonald, I. T., & Vincent, C. E. (2014). Modelling acoustic scattering by suspended flocculating sediments. *Continental Shelf Research*, *88*, 81–91. https://doi.org/10.1016/j.csr.2014.07.003
Thorne, P. D., & Meral, R. (2008). Formulations for the scattering properties of suspended sandy sediments for use in the application of acoustics to sediment transport processes. *Continental Shelf Research*, *28*(2), 309–317. https://doi.org/10.1016/j.csr.2007.08.002
Topping, D. J., Rubin, D. M., Wright, S. A., & Melis, T. S. (2011). Field evaluation of the error arising from inadequate time averaging in the standard use of depth-integrating suspended-sediment samplers. In *USGS professional paper 1774*.
Topping, D. J., & Wright, S. A. (2016). Long-term continuous acoustical suspended-sediment measurements in rivers—Theory, application, bias, and error. In *USGS professional paper 1823*. https://doi.org/10.3133/pp1823
Topping, D. J., Wright, S. A., Melis, T. S., & Rubin, D. M. (2007). High-resolution measurements of suspended-sediment concentration and grain size in the Colorado River in Grand Canyon using a multi-frequency acoustic system. In *Proceedings of the 10th international symposium on river sedimentation, Russia, Moscow*.
Tuthill, T. A., Sperry, R. H., & Parker, K. J. (1988). Deviations from Rayleigh statistics in ultrasonic speckle. *Ultrasonic Imaging*, *10*(2), 81–89. https://doi.org/10.1177/016173468801000201
Urick, R. J. (1948). The absorption of sound in suspensions of irregular particles. *Journal of the Acoustical Society of America*, *20*(3), 283–289. https://doi.org/10.1121/1.1906373
Venditti, J. G., Church, M., Attard, M. E., & Haught, D. (2016). Use of ADCPs for suspended sediment transport monitoring: An empirical approach. *Water Resources Research*, *52*(4), 2715–2736. https://doi.org/10.1002/2015wr017348

Vergne, A., Berni, C., Le Coz, J., & Tencé, F. (2021). Acoustic backscatter and attenuation due to river fine sediments: Experimental evaluation of models and inversion methods. *Water Resources Research*, *57*(9), e2021WR029589. https://doi.org/10.1029/2021WR029589

Vergne, A., Le Coz, J., & Berni, C. (2023). *Supplementary information of the research paper Vergne et al. (2023)*. Recherche Data Gouv. https://doi.org/10.57745/SGADUP

Vergne, A., Le Coz, J., Berni, C., & Pierrefeu, G. (2020). Using a down-looking multifrequency ABS for measuring suspended sediments in rivers. *Water Resources Research*, *56*(2), e2019WR024877. https://doi.org/10.1029/2019wr024877

Vincent, C. E., Hanes, D. M., & Bowen, A. J. (1991). Acoustic measurements of suspended sand on the shoreface and the control of concentration by bed roughness. *Marine Geology*, *96*(1–2), 1–18. https://doi.org/10.1016/0025-3227(91)90199-e

Vincent, C. E., & MacDonald, I. T. (2015). A flocculi model for the acoustic scattering from flocs. *Continental Shelf Research*, *104*, 15–24. https://doi.org/10.1016/j.csr.2015.05.002

Wright, S. A., Topping, D. J., & Williams, C. A. (2010). Discriminating silt-and-clay from suspended-sand in rivers using side-looking acoustic profilers. In *Proceedings of the 2nd joint federal interagency sedimentation conference, USA, Las Vegas*.